CERN - DATA HANDLING DIVISION
DD/75/2
D.W. Townsend
J.D. Wilson
January 1975

The Quintic Spline for Momentum Determination in Omega

The Quintic Spline for Momentum Determination in Omega

D.W. Townsend & J.D. Wilson

Abstract

A quintic spline model for the trajectory of a particle in a magnetic field is compared with the conventional field-dependent helix fit, using both real and simulated data.

The same accuracy in the estimates of the track parameters is obtained significantly faster by the spline model than the conventional fit.

In addition, the model is successfully applied to simulated data at SPS energies.

1. Introduction

This report describes the use of a quintic spline model for fitting particle trajectories in the Omega spectrometer. Position measurements are made along the trajectories using optical spark chambers with plumbicon camera readout. The chambers are placed within the 18 kgauss, superconducting, Omega magnet and are of two types: eight modules (ten gaps/module), perpendicular to the beam direction, downstream of the target; eight modules (eight gaps/module), parallel to the target with four modules on each side. This layout is shown schematically in the diagram below.

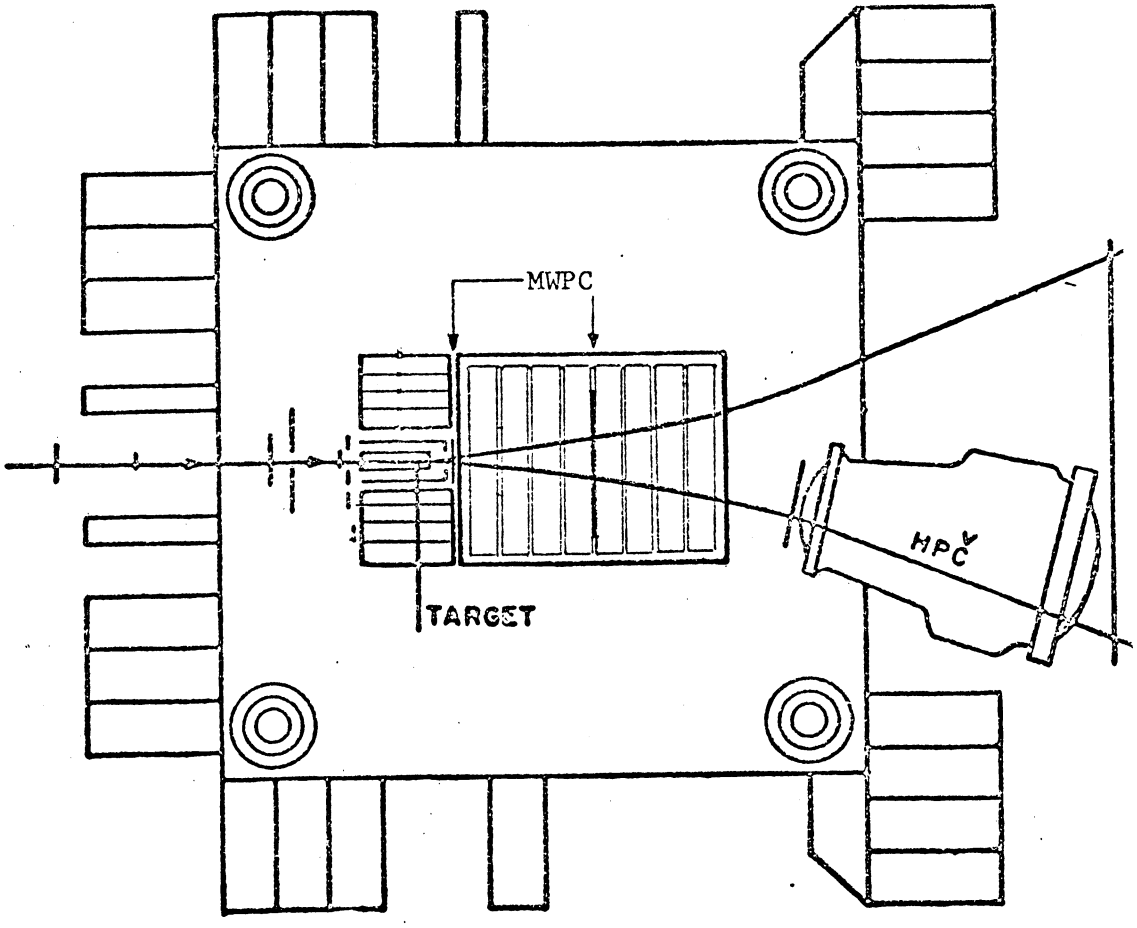

Schematic layout of Omega

A complete off-line track recognition and geometry analysis program, ROMEO, was written to process the data from the Omega. The geometry analysis is based on a conventional, field-dependent helix fit to the measurements

in order to determine the track momentum (p) and direction (λ, ϕ) at the first measured point, and ultimately at the interaction vertex. As an alternative to the helix fit, the quintic spline model proposed by H. Wind[1] is used and the results compared.

This model uses a cubic spline representation of the magnetic field, which is therefore discontinuous in the third derivative. The track model is consequently a quintic spline, since the curvature (which is given by the field representation) is essentially the second derivative of the track.

A program to fit such a model has been written[2] and its performance on both real and simulated data is described. In addition, the use of spline fits for momentum determination in Omega at SPS energies is discussed in the last section. Momentum estimates obtained from a combination of points both inside and outside the magnetic field is considered using simulated data at 100 GeV/c.

2. Interface into ROMEO

The final fit to the track points in the case of the spline routine is made in two orthogonal projections that are obtained from the original space coordinate system by a simple rotational transformation. This transformation is to make the slope of the track (y' and z') at each point as small as possible (y', z' < 1). To obtain this transformation it is of course necessary to first reconstruct the track in space, and therefore the spline fit has been inserted into ROMEO immediately following the reconstruction of the space points on each track. It replaces both the initial, constant field, helix fit and the final field-dependent integration.

In order to use the track parameters output from the spline fit, a modification to obtain the errors on these parameters was necessary. These errors are used in ROMEO in the extrapolation of the tracks to the vertex.

As explained in ref. 1, the final fit to obtain the track parameters a_1, b_1 (position of first point), a_2, b_2 (slope at first point) and momentum p, reduces to:

$$y_i = a_1 + a_2 x_i + d\, Y(x_i)$$
$$z_i = b_1 + b_2 x_i + d\, Z(x_i) \qquad i = 1 \ldots N \text{ , for N measurements.}$$

where $d = \frac{1}{p}$, and $Y(x_i)$, $Z(x_i)$ are quintic spline functions that depend on the magnetic field, y' and z'. If the fit is done simultaneously in the two projections, the normal equations of the least squares fit are given by:

$$\underset{\approx}{A}\underset{\sim}{X} = \underset{\sim}{B}$$

with:

$$X = \begin{pmatrix} a_1 \\ a_2 \\ d \\ b_1 \\ b_2 \end{pmatrix} \qquad B = \begin{pmatrix} \Sigma y \\ \Sigma xy \\ \Sigma Yy + \Sigma Zz \\ \Sigma z \\ \Sigma xz \end{pmatrix}$$

and

$$A = \begin{pmatrix} N & \Sigma x & \Sigma Y & 0 & 0 \\ \Sigma x & \Sigma x^2 & \Sigma xY & 0 & 0 \\ \Sigma Y & \Sigma xY & \Sigma Y^2 + \Sigma Z^2 & \Sigma Z & \Sigma xZ \\ 0 & 0 & \Sigma Z & N & \Sigma x \\ 0 & 0 & \Sigma xZ & \Sigma x & \Sigma x^2 \end{pmatrix}$$

The least squares solution is given by:

$$\underset{\sim}{X} = \underset{\approx}{A}^{-1}\underset{\sim}{B}$$

and the error matrix of the parameters $\underset{\sim}{X}$ by:

$$\mathrm{cov}(\underset{\sim}{X}) = \underset{\approx}{A}^{-1}$$

The form of $\underset{\approx}{A}$ is such that the inversion may be written down explicitly. This procedure is used in the program (ref. 2) and leads to the solutions:

$$\left.\begin{aligned} \frac{1}{p} &= \{t_3^2\,(\Sigma yY + \Sigma zZ) - t_3(t_1\Sigma Y + t_4\Sigma xY) - t_3(t_7\Sigma z + t_{10}\Sigma xZ)\}\,/D \\ a_1 &= (t_1 - \tfrac{1}{p}\cdot t_2)/t_3 \\ a_2 &= (t_4 - \tfrac{1}{p}\cdot t_5)/t_3 \\ b_1 &= (t_7 - \tfrac{1}{p}\cdot t_8)/t_3 \\ b_2 &= (t_{10} - \tfrac{1}{p}\cdot t_{11})/t_3 \end{aligned}\right\} \quad (1)$$

where the t_i are given by:

$$t_1 = \Sigma x^2\,\Sigma y - \Sigma x \Sigma xy \qquad t_8 = \Sigma x^2 \Sigma Z - \Sigma x \Sigma xZ$$
$$t_2 = \Sigma Y \Sigma x^2 - \Sigma xY \Sigma x \qquad t_{10} = -\Sigma x \Sigma z + N\,\Sigma xz$$
$$t_3 = N\Sigma x^2 - \Sigma x\,\Sigma x \qquad t_{11} = -\Sigma Z \Sigma x + N\,\Sigma xZ$$
$$t_4 = -\Sigma x \Sigma y + N \Sigma xy$$
$$t_5 = -\Sigma Y \Sigma x + N \Sigma xY$$
$$t_7 = \Sigma x^2 \Sigma z - \Sigma x \Sigma xz$$

and $D = \mathrm{Det}(\underset{\approx}{A})$

$$= \{t_3^2(\Sigma Y^2 + \Sigma Z^2) - t_3(t_2 \Sigma Y + t_5 \Sigma xY) - t_3(t_8 \Sigma Z + t_{11} \Sigma xZ)\}$$

The modification to the spline routine in order to determine the actual elements of the inverse of the matrix $\underset{\approx}{A}$ is straightforward once the above expressions have been calculated. Note that the summations are in all cases the *weighted* sums e.g.

$$\Sigma x \equiv \sum_{i=1}^{N} w_i x_i \ ,$$

where w_i is the weight of the ith point. In particular $\sum_{i=1}^{N} w_i = N$ for an unweighted fit.

Thus, by writing down the solution, for example, for the parameter $1/p$ in terms of the elements of $\underset{\approx}{A}^{-1}$ and equating coefficients with equations(1), the elements of $\underset{\approx}{A}^{-1}$ appearing in the expression for $\frac{1}{p}$ may be explicitly defined in terms of the t_i and D. Similarly for a_1, a_2, etc. so as to give:

$$A^{-1} = \frac{1}{D} \begin{bmatrix} \Sigma x^2 \cdot D/t_3 + t_2^2 & -\Sigma x \cdot D/t_3 + t_2 t_5 & -t_2 \cdot t_3 & t_2 \cdot t_8 & t_2 \cdot t_{11} \\ -\Sigma x \cdot D/t_3 + t_2 t_5 & N \cdot D/t_3 + t_5^2 & -t_5 \cdot t_3 & t_5 \cdot t_8 & t_5 \cdot t_{11} \\ -t_2 \cdot t_3 & -t_5 \cdot t_3 & t_3^2 & -t_3 \cdot t_8 & -t_3 \cdot t_{11} \\ +t_2 \cdot t_8 & +t_5 \cdot t_8 & -t_3 \cdot t_8 & \Sigma x^2 \cdot D/t_3 + t_8^2 & -\Sigma x \cdot D/t_3 + t_8 t_{11} \\ +t_2 \cdot t_{11} & t_5 \cdot t_{11} & -t_3 \cdot t_{11} & -\Sigma x \cdot D/t_3 + t_8 t_{11} & N \cdot D/t_3 + t_{11}^2 \end{bmatrix} \qquad (2)$$

The elements of this matrix give the errors on the parameters a_1, a_2, b_1', b_2 and $\frac{1}{d}$, and the correlations between them. In order to obtain *absolute* errors it is necessary to put the true weights of the points in the summations appearing in the t_i, and not simply the *relative* weights.

The simplest approximation is to assume that all the measurements are independent and do not depend on either position along the track or absolute position in space. All points then have equal weight in the fit, and the weight matrix is diagonal with elements:

$$W_{ij} = \frac{1}{\sigma^2} \qquad i = j$$
$$W_{ij} = 0 \qquad i \neq j$$

where σ is the absolute error assigned to each measured point. The absolute errors on the parameters are then given by the elements of $\underset{\approx}{A}^{-1}$ scaled by σ.

$$\text{e.g.} \quad \sigma^2_{a_1} = \sigma^2 \{ \frac{1}{t_3} \cdot \sum_{i=1}^{N} x_i^2 + t_2^2/D \} \quad , \qquad \text{etc.}$$

Then, in the absence of an exact calculation of the weight matrix, it is usual to choose σ in one of two ways:

a) As a constant for the given measurement system. In this case σ does not vary from point to point or track to track. It gives no indication whether a track is well or badly measured, and is in any case difficult to estimate for a complex measuring device such as the Omega.

b) As a function of the fitted track residuals. It is shown in ref. 3 that an *unbiased* estimator of σ^2 is given by:

$$\hat{\sigma}^2 = Q^2_{min}/(N - r)$$

where r is the number of parameters fitted (= 5) and Q^2_{min} is the final sum of squares of the residuals, summed over all measurements.

The second method is used by ROMEO in the conventional helix fit and extended to the spline routines, where:

$$Q^2_{min} = S^2_{xy} + S^2_{xz}, \quad S_{xy(xz)} = \text{residual sum in xy(xz) projection.}$$

i.e. summed over both projections, xy and xz.

The parameters a_1, a_2, b_1, b_2 and their errors are expressed in the rotated system. In order to obtain the usual track parameters λ_o, ϕ_o y_o and z_o at the first measured point x_o, together with their errors, it is necessary to apply the inverse coordinate transformation, and use the normal rule for the combination of errors.

The error calculations may be simplified by neglecting the off-diagonal elements of the transformation matrix. In practice, for tracks with momenta greater than a few GeV/c and small production angles this initial rotation may be omitted completely[4], so that all the fitting is done in the original space coordinate system.

2.1 Non-Diagonal Weight Matrix

The field-dependent helix fit in ROMEO is unweighted, i.e. all the measurements have equal, unit weight, and the weight matrix is diagonal. As mentioned above, the spline routine allows the possibility of giving each measurement a different weight, but still assumes a diagonal weight matrix.

The inclusion of a full weight matrix in the spline fit has been studied[4,5] for the purpose of treating multiple scattering and energy loss. It turns out to be straightforward, once the full weight matrix has been calculated. The matrix of the normal equations $(\underset{\approx}{A})$ then has to be explicitly inverted for each track since it does not have the simple form of the uncorrelated case that gives the solutions of eqns. (1).

For the purposes of this comparison with ROMEO, all points fitted by the spline are assumed to have equal, unit weight.

2.2 Estimate of First Derivatives

In the standard quintic spline routine, the estimates of the first derivatives y' and z' at each measured point on the track are obtained from

a preliminary cubic spline fit. In some cases, better estimates may be obtained from a preliminary circle fit (in xy) and straight line fit (in xz). This procedure therefore makes use *a priori* of information about the track (that it is approximately circular in the xy plane, etc.) and has the advantage of smoothing the effect of the experimental errors on the initial estimates of y' and z'. Further improvement could be obtained by using the actual magnetic field at each point in the preliminary fit, since it is needed for the final fit in any case.

In addition, there is the possibility of iterating in the final fit by using the values of y" and z" in order to estimate improved values of y' and z'. This procedure should converge provided y' and z' are small, and in particular less than unity. The initial coordinate transformation may be omitted only if this condition on y' and z' is already satisfied in the original system, otherwise the iteration may diverge.

3. Comparison with ROMEO for Real and Simulated Data

For the purpose of comparing the spline method with the field-dependent helix fit method on a track by track basis, the ROMEO Geometry program was modified, as described above, to allow each track to be reconstructed independently by the two methods. The parameters from the spline fit were then put in the form required by ROMEO so that direct comparisons could be made in histogram form. The parameters chosen for comparison were the total absolute momentum ($p \equiv 1/d$), the dip angle ($\lambda \equiv \arctan(b_2)$) and the azimuthal angle ($\phi \equiv \arctan(a_2)$) at the first point on the track. Tracks with less than six points, or which could not be reconstructed by ROMEO were not compared, and do not appear in the histogram.

3.1 Real Data

A sample of 5000 tracks from an experiment to study reactions of the type $\pi^- p \to pX^-$ at 12 GeV/c incident beam momentum was used. The results are shown in the two-dimensional histograms of Fig. 1. The diagonal line drawn in each plot corresponds to ROMEO and the spline giving the same value for p, λ or ϕ. As can be seen, the parameters from the spline fit show very good agreement with those from ROMEO with no obvious systematic bias. The few points a long way off the diagonal line have been investigated and found to come from tracks with one or more wrong points assigned by

the Pattern Recognition part of ROMEO. These tracks may give wrong results in the ROMEO fit or the spline fit or both, and can affect the two types of fit in different ways.

3.2 Simulated Data

In order to compare the parameters with their 'true' values, a sample of simulated data was generated. 100 events of the type $\gamma p \rightarrow \rho' p$, $\rho' \rightarrow 4\pi$, with 12 GeV incident γ were used, giving secondary tracks up to a momentum of about 7 GeV/c. Two-dimensional histograms were plotted of the quantities:

$$(p_{SPLINE} - p_{TRUE})/p_{TRUE} \text{ vs } p_{TRUE}$$

$$(p_{ROMEO} - p_{TRUE})/p_{TRUE} \text{ vs } p_{TRUE}$$

$$(p_{SPLINE} - p_{ROMEO})/p_{TRUE} \text{ vs } p_{TRUE}$$

and the results are shown in Fig. 2.

A bias of about 0.1% is seen in the $p_{SPLINE} - p_{ROMEO}$ distribution (Fig. 2c), which is almost entirely due to a bias in the ROMEO fit as seen by comparing Figs. 2a and 2b. The $p_{SPLINE} - p_{ROMEO}$ distribution can also be seen to be much narrower than the other two distributions, showing that both fits generally give the same result.

The differences in angle, $\lambda_{SPLINE} - \lambda_{ROMEO}$ and $\phi_{SPLINE} - \phi_{ROMEO}$, are shown in Figs. 3 and 4. They are both well centred on zero to better than 0.1 mrad.

As can be seen from Figs. 2a and 2b, some tracks with momenta less than a few hundred MeV/c can be badly fitted by either or both methods. In addition, the presence of tails to the distributions in Figs. 2c, 3 and 4 indicates that these low momentum tracks can give different results for the two methods in the same way as the badly associated points in the case of real data (section 3.1). In general, a track that is badly fitted in either ROMEO or the spline fit results in poor (and different) values for all these parameters p, λ and ϕ. The same track will then appear in the tails of all the distributions shown in Figs. 2, 3 and 4.

3.3 Accuracy

The results from the spline fit given in the previous sections were obtained using a cubic spline estimate for the first derivatives. No obvious improvement was obtained in the final result by replacing the cubic spline with circle and straight line fits, as discussed in section 2.2.

However, a noticeable improvement was found when *two* iterations of the spline were made, but more than two iterations produced no further improvement. Since the spline uses the reconstructed space points, the field needs to be looked up only during the first iteration. Subsequent iterations simply improve the estimates of the first derivatives. It is even possible that the spline could achieve the same accuracy with *fewer* field calls than at every measurement (e.g. in 15 cm steps instead of 5 cm - the mean space point separation). This is because the field representation for the helix fit is step-wise with a discontinuity at the end of each step. This leads to a second order spline for the track, which could be expected to be less realistic than the quintic spline track model.

On the other hand ROMEO looks up the field not at the reconstructed space points, but at points estimated from the parameters of the initial helix fit and the corresponding arc length. Tracks for which these initial parameters are far from their true values require at least two iterations of the final fit, but with the magnetic field looked up in each iteration. The above comparisons were made for two iterations of the spline and *at least two* iterations in ROMEO (until the fit 'converged').

3.4 Timings

The processing time for a given track depends on the number of points to be fitted and the number of iterations to achieve the required accuracy. The same sample of events was processed by both methods, allowing first one iteration and then two. The results, for a CDC 7600 are given in the table below:

	No. of Iterations	Time/Track (msecs)
ROMEO	1	8.1
	2	13.2
SPLINE	1	2.9
	2	3.5

The large increase in the ROMEO time compared with the spline when going from one to two iterations is due to the fact that for ROMEO the field is looked up in each iteration (see section 3.3).

The overall time/event will depend on the fraction of tracks for which more than one ROMEO iteration is necessary. However, even with only a single ROMEO iteration, the spline could speed up the Geometry processing time by a factor of about 2 for a typical 4-track event.

4. Extension to Higher Momentum

The spline fit was tested using simulated data with an incident beam momentum of 100 GeV/c. No unexpected deterioration or bias in the momentum estimates was observed up to the maximum momentum of the secondary tracks. In Fig. 5, the fitted and simulated values of momentum are compared as a function of the simulated momentum.

All the above results, both for real and simulated data, have been for tracks measured entirely *inside* the magnetic field, in a region where the field is uniform to $\sim$ 15% to 20%. In order to provide the necessary momentum resolution at high energies, spectrometers such as Omega will be equipped with some downstream chambers in zero or low field regions, outside the magnet. The momentum of the fast tracks will be determined by a fit to points both inside and outside the field. This may readily be done with the spline fit, but some care is necessary when inserting extra field points, as the following example shows.

An entirely fictional layout such as in Fig. 6 was tested with tracks of momenta up to 100 GeV/c. Five 'modules', each giving an unambiguous space point, were used, two inside and three outside the field. The

results of using the spline fit to estimate the momentum is summarised in Fig. 7. In each case the diagram on the right shows the $\Delta p/p$ (%) comparing the fitted and simulated momenta for a sample of tracks, and the diagram on the left shows the cubic spline fit to the magnetic field (for a "typical" track) compared with the actual field distribution used in the simulation.

In Fig. 7a, no extra field points are inserted between the measurements, resulting in a $\sim$ 30% bias in the momentum estimate ($p_{SPLINE} > p_{TRUE}$), due to the overestimate of the field integral. Five extra field calls between chambers 2 and 3 reduces this bias to about 3% (Fig. 7b). Ten extra points however *increases* this bias to $\sim$ 4%, because of a worse fit to the field in the sensitive region between chambers 1 and 2 (Fig. 7c). Five points between 1 and 2, and five between 2 and 3 eliminates this bias almost completely (Fig. 7d), even though the simulated field distribution did not really satisfy the implicit assumption that the field is smooth and satisfies Maxwell's Equations.

Although, for this simple example, the result is rather obvious, the point to be made is that biases in the momentum estimate from the spline may easily be introduced unless the magnetic field is correctly represented. These and subsequent tests have led to the conclusion that there is no evidence for any inherent bias due to the method.

Biases of a similar type have been observed in other applications of the spline fit[6], but for the examples given above there is no reason to believe that such biases cannot be removed by a careful choice of extra field calls.

Acknowledgement

We should like to thank H. Wind for his interest and helpful advice.

References

1. Momentum analysis by using a quintic spline model for the track.
H. Wind, Nucl. Inst. and Methods 115 (1974), p. 431.

2. CERN Program Library, X510. B.J. Braams.

3. Statistical methods in experimental physics. W.T. Eadie, D. Drijard,
F.E. James, M. Roos, B. Sadoulet. North Holland Publishing Co., Section 8.4.

4. Private communication. A. Frohlich.

5. Treatment of multiple scattering and energy loss for quintic splines.
LMOS Note 34 (1974).

6. A look at spline fits. D.B. Smith, LMOS Note 32 (1974).

Figure Captions

1a.	p_{SPLINE} vs p_{ROMEO} . Momentum	Real Data.
1b.	λ_{SPLINE} vs λ_{ROMEO} . Dip Angle	
1c.	ϕ_{SPLINE} vs ϕ_{ROMEO} . Azimuthal Angle	
2a.	$(p_{ROMEO} - p_{TRUE})/p_{TRUE}$ vs p_{TRUE}	Simulated Data.
2b.	$(p_{SPLINE} - p_{TRUE})/p_{TRUE}$ vs p_{TRUE}	
2c.	$(p_{SPLINE} - p_{ROMEO})/p_{TRUE}$ vs p_{TRUE}	
3.	Dip Angle: $\lambda_{SPLINE} - \lambda_{ROMEO}$	Simulated Data.
4.	Azimuthal Angle: $\phi_{SPLINE} - \phi_{ROMEO}$	
5.	$(p_{SPLINE} - p_{TRUE})/p_{TRUE}$ vs p_{TRUE}	Simulated Data. 100 GeV/c.
6.	Layout of chambers for 100 GeV/c simulation.	
7a. 7b. 7c. 7d.	Fitted magnetic field distribution and $(p_{SPLINE} - p_{TRUE})/p_{TRUE}$	For inserted points.

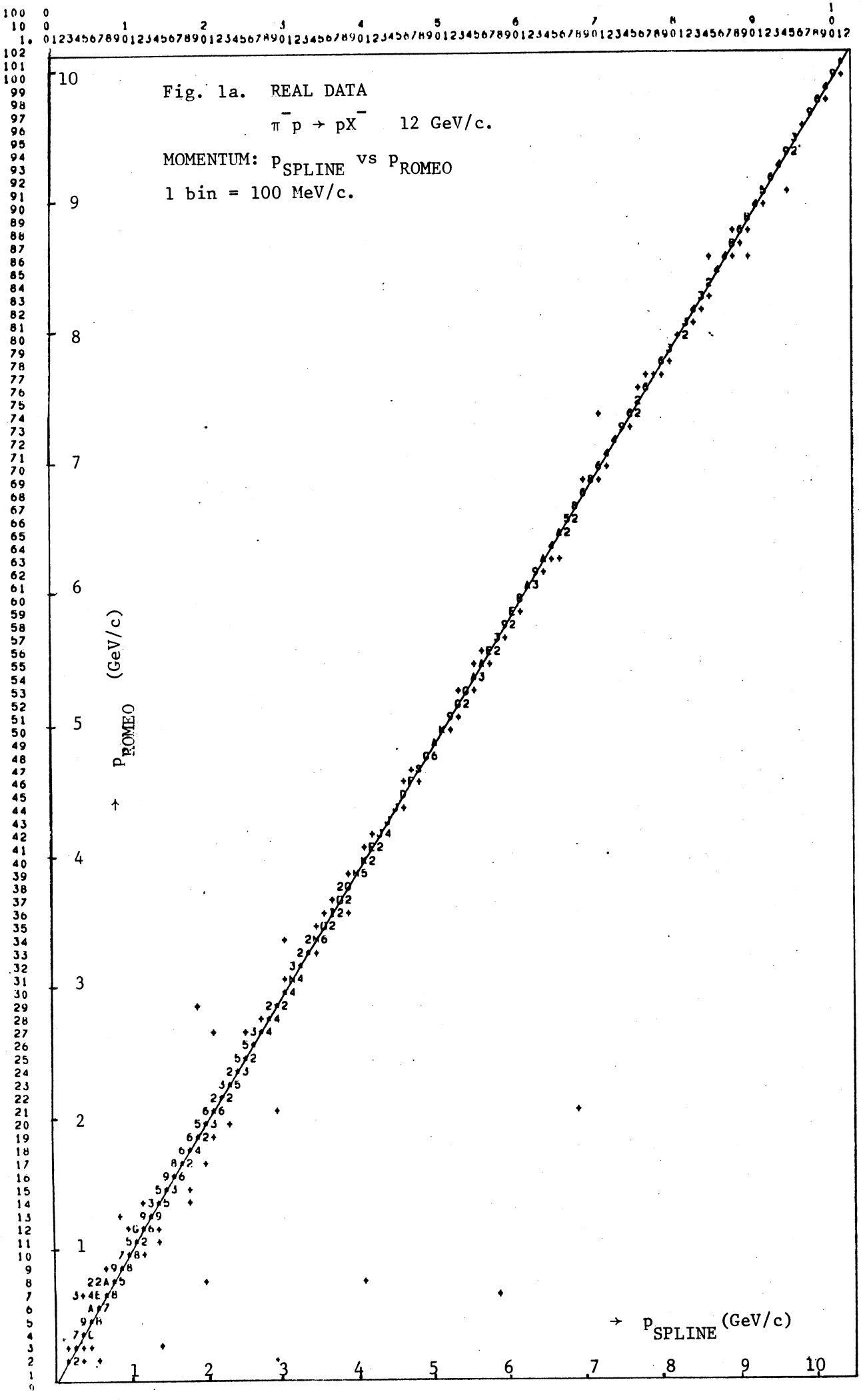
Fig. 1a. REAL DATA
$\pi^- p \rightarrow pX^-$ 12 GeV/c.
MOMENTUM: p_{SPLINE} vs p_{ROMEO}
1 bin = 100 MeV/c.
p_{ROMEO} (GeV/c)
p_{SPLINE} (GeV/c)

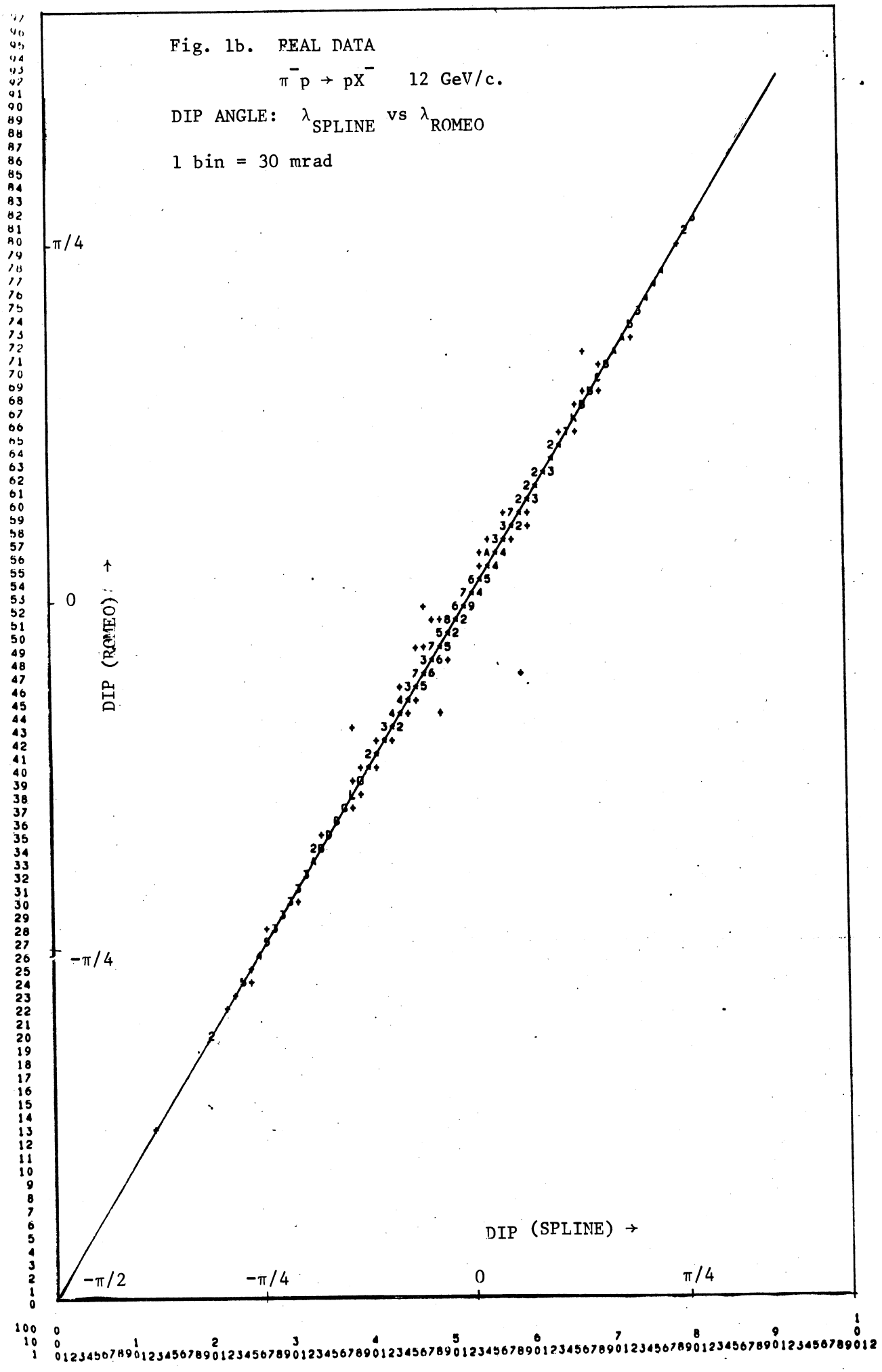
Fig. 1b. REAL DATA
$\pi^- p \rightarrow pX^-$ 12 GeV/c.
DIP ANGLE: λ_{SPLINE} vs λ_{ROMEO}
1 bin = 30 mrad
π/4
0
-π/4
DIP (ROMEO) →
DIP (SPLINE) →
-π/2
-π/4
0
π/4

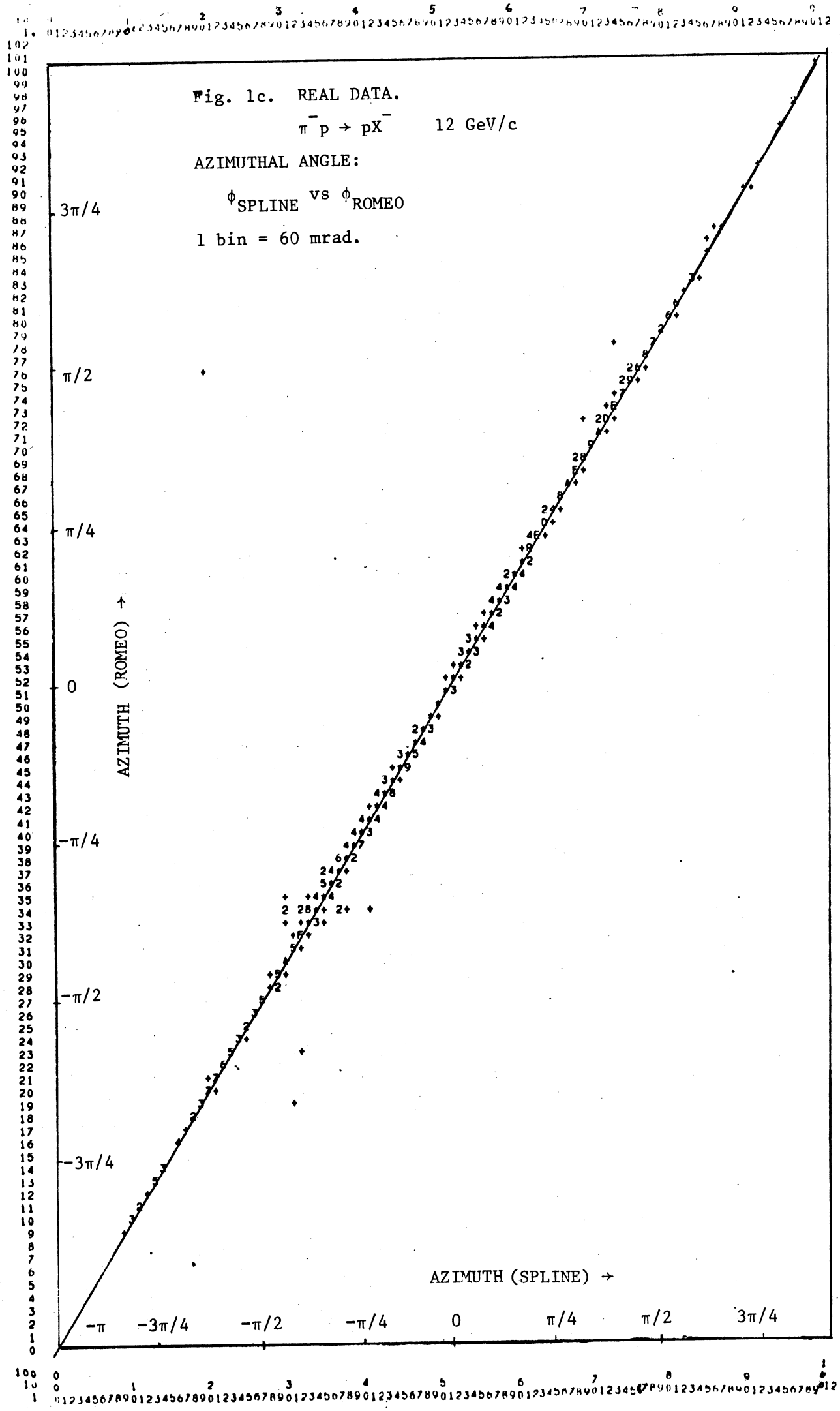
Fig. 1c. REAL DATA.
$\pi^- p \rightarrow pX^-$ 12 GeV/c
AZIMUTHAL ANGLE:
ϕ_{SPLINE} vs ϕ_{ROMEO}
1 bin = 60 mrad.
3π/4
π/2
π/4
0
-π/4
-π/2
-3π/4
AZIMUTH (ROMEO) →
AZIMUTH (SPLINE) →
-π
-3π/4
-π/2
-π/4
0
π/4
π/2
3π/4

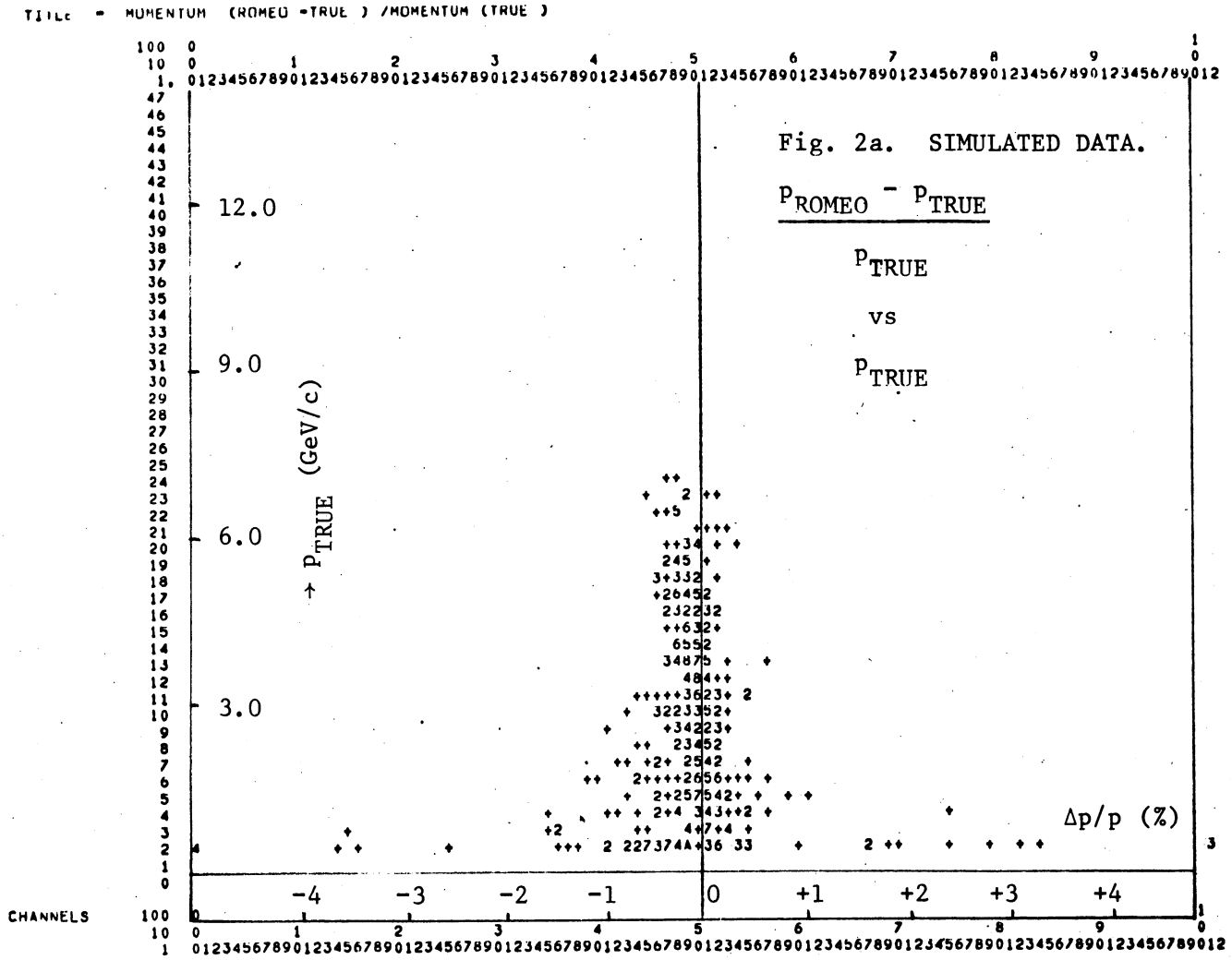

Fig. 2a. SIMULATED DATA.

$$\frac{p_{ROMEO} - p_{TRUE}}{p_{TRUE}} \text{ vs } p_{TRUE}$$

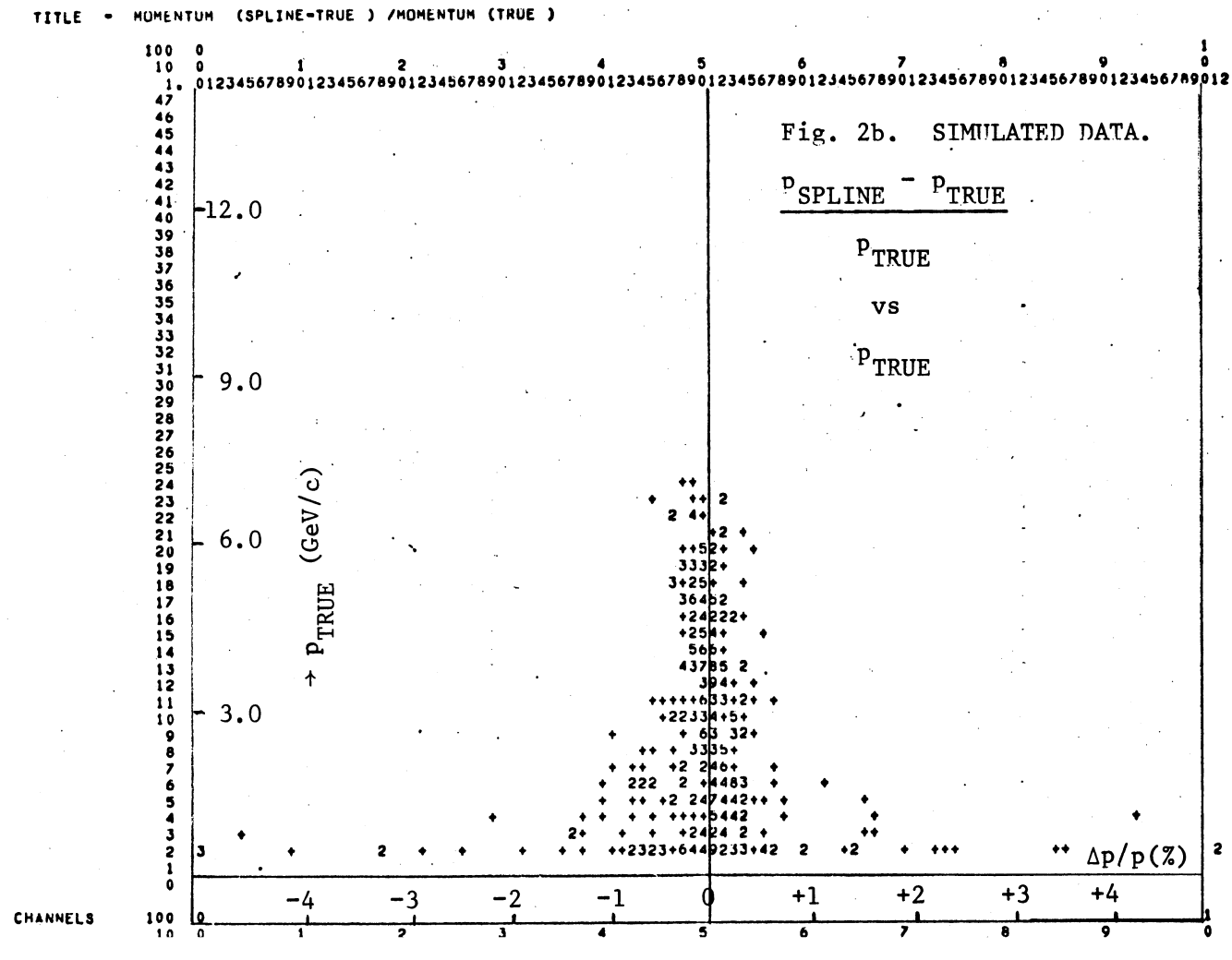

Fig. 2b. SIMULATED DATA.

$$\frac{p_{SPLINE} - p_{TRUE}}{p_{TRUE}} \text{ vs } p_{TRUE}$$

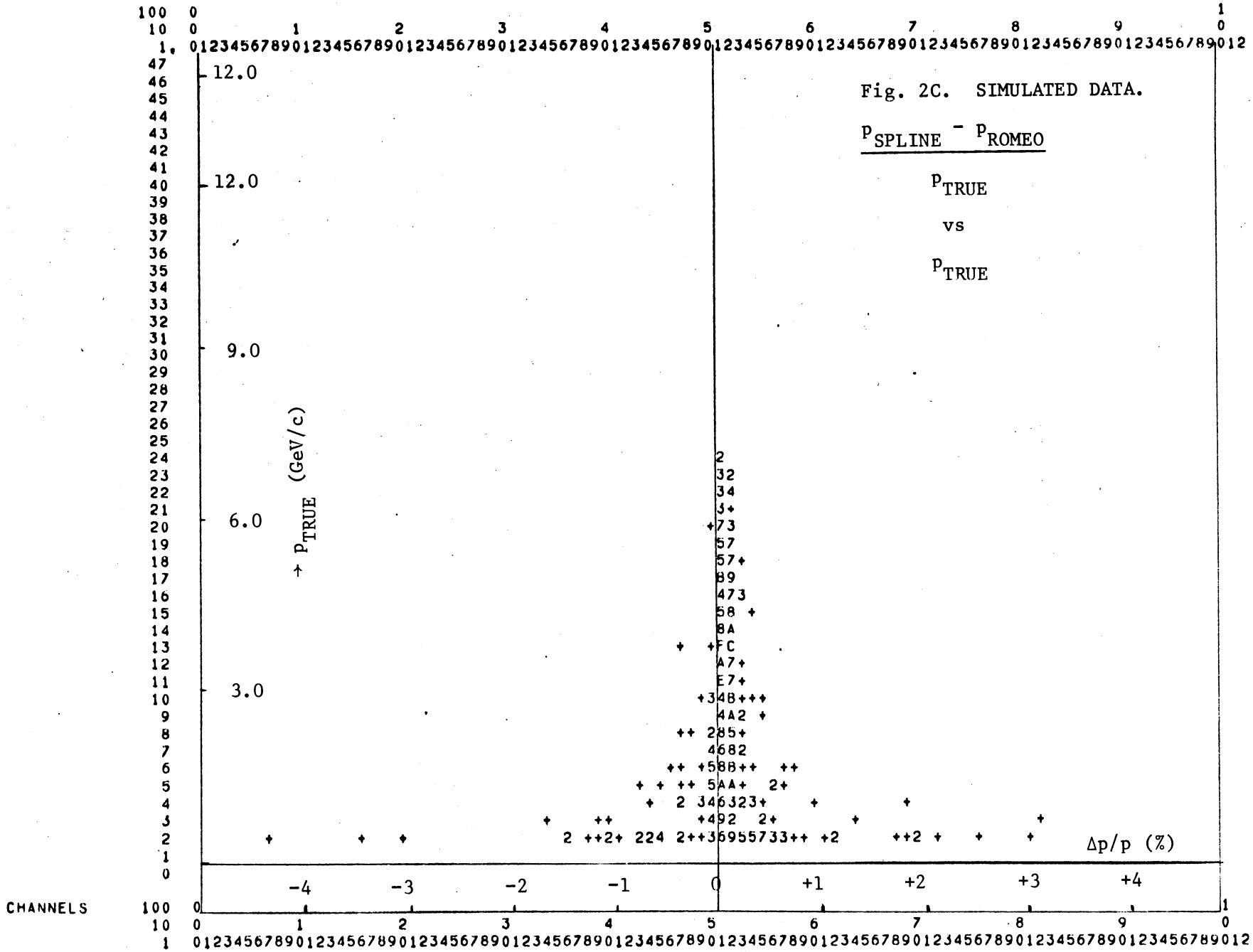

Fig. 2C. SIMULATED DATA.

$\frac{p_{SPLINE} - p_{ROMEO}}{p_{TRUE}}$ vs p_{TRUE}

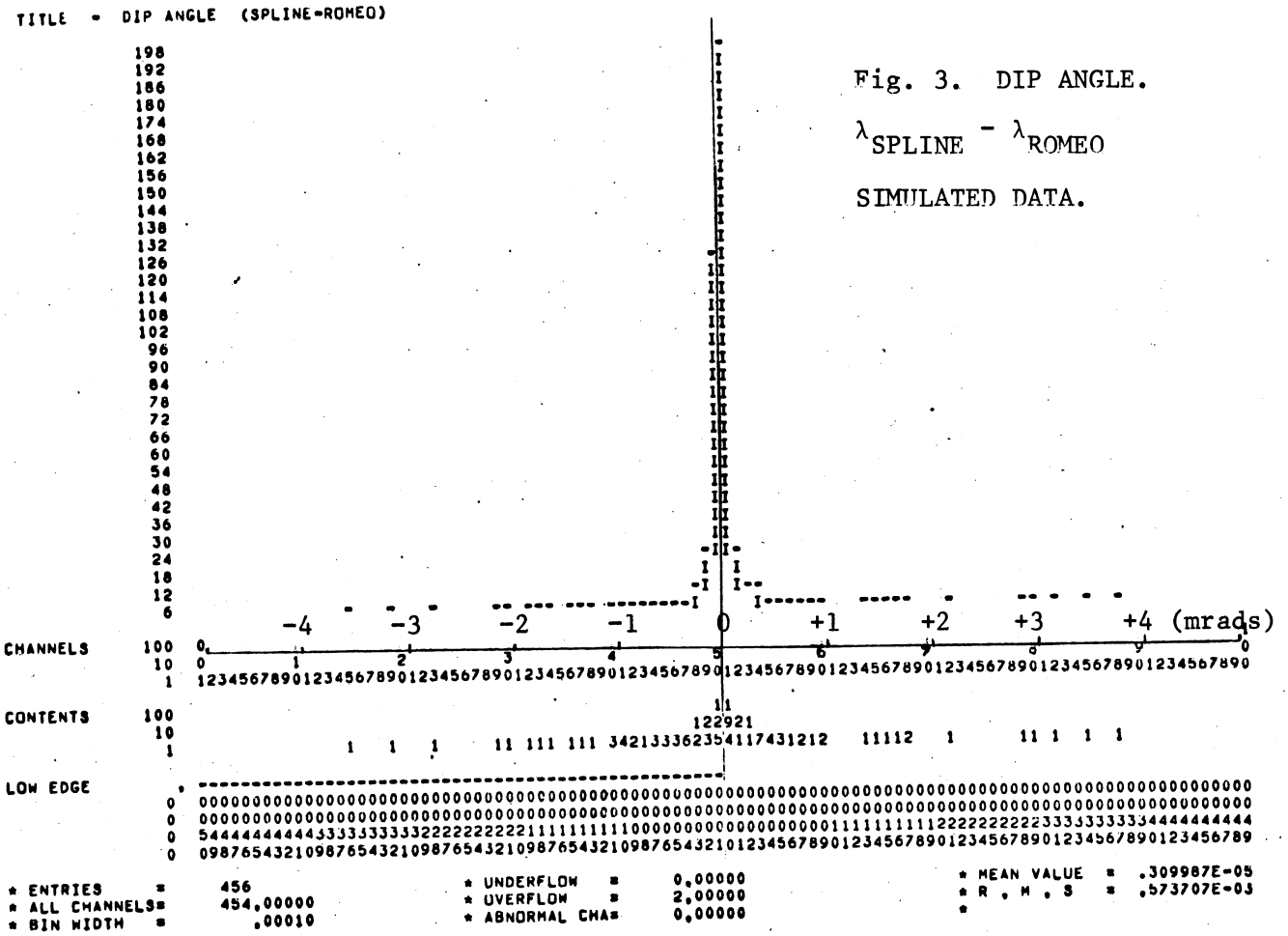

Fig. 3. DIP ANGLE.

$\lambda_{SPLINE} - \lambda_{ROMEO}$

SIMULATED DATA.

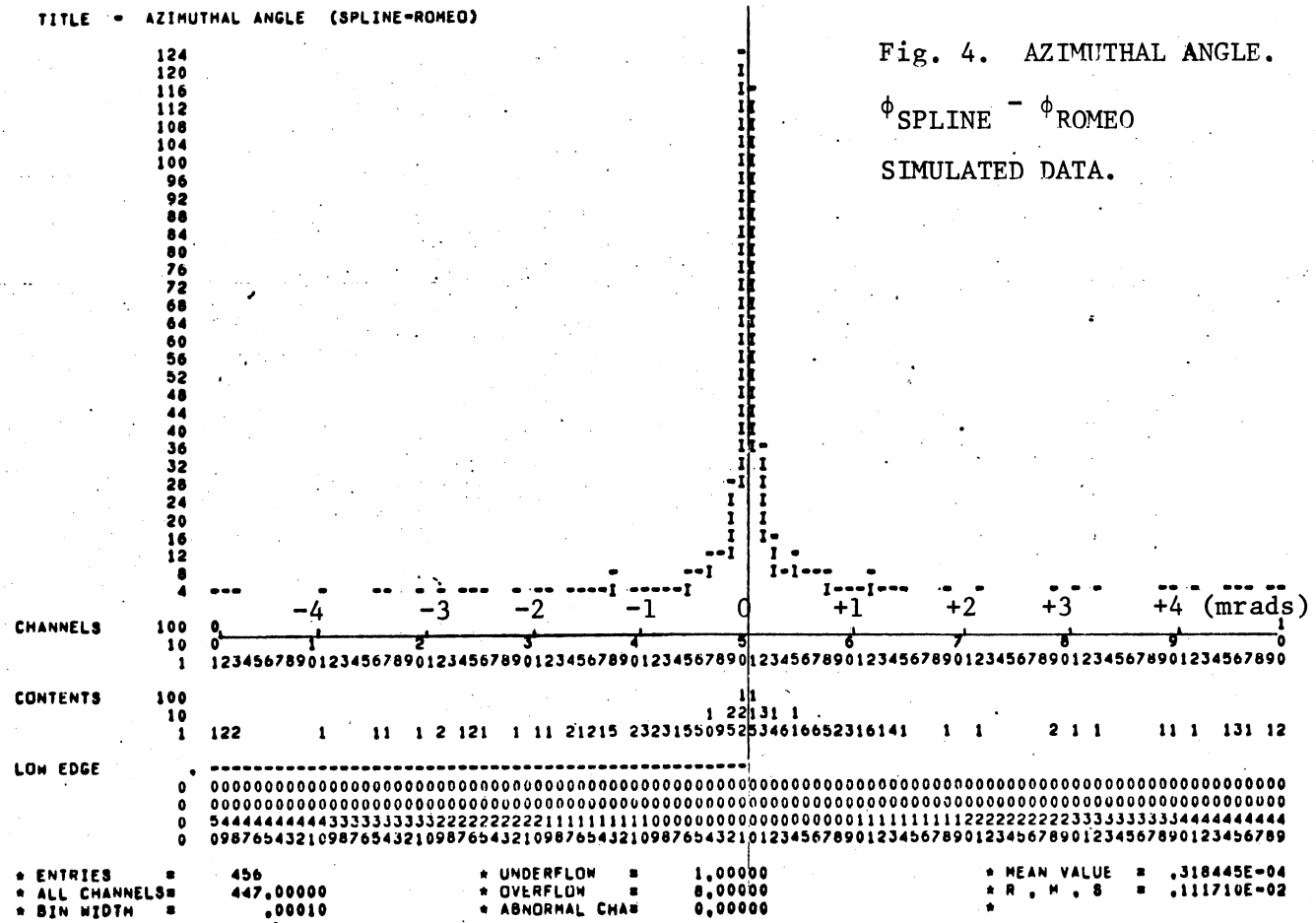

Fig. 4. AZIMUTHAL ANGLE.

$\phi_{SPLINE} - \phi_{ROMEO}$

SIMULATED DATA.

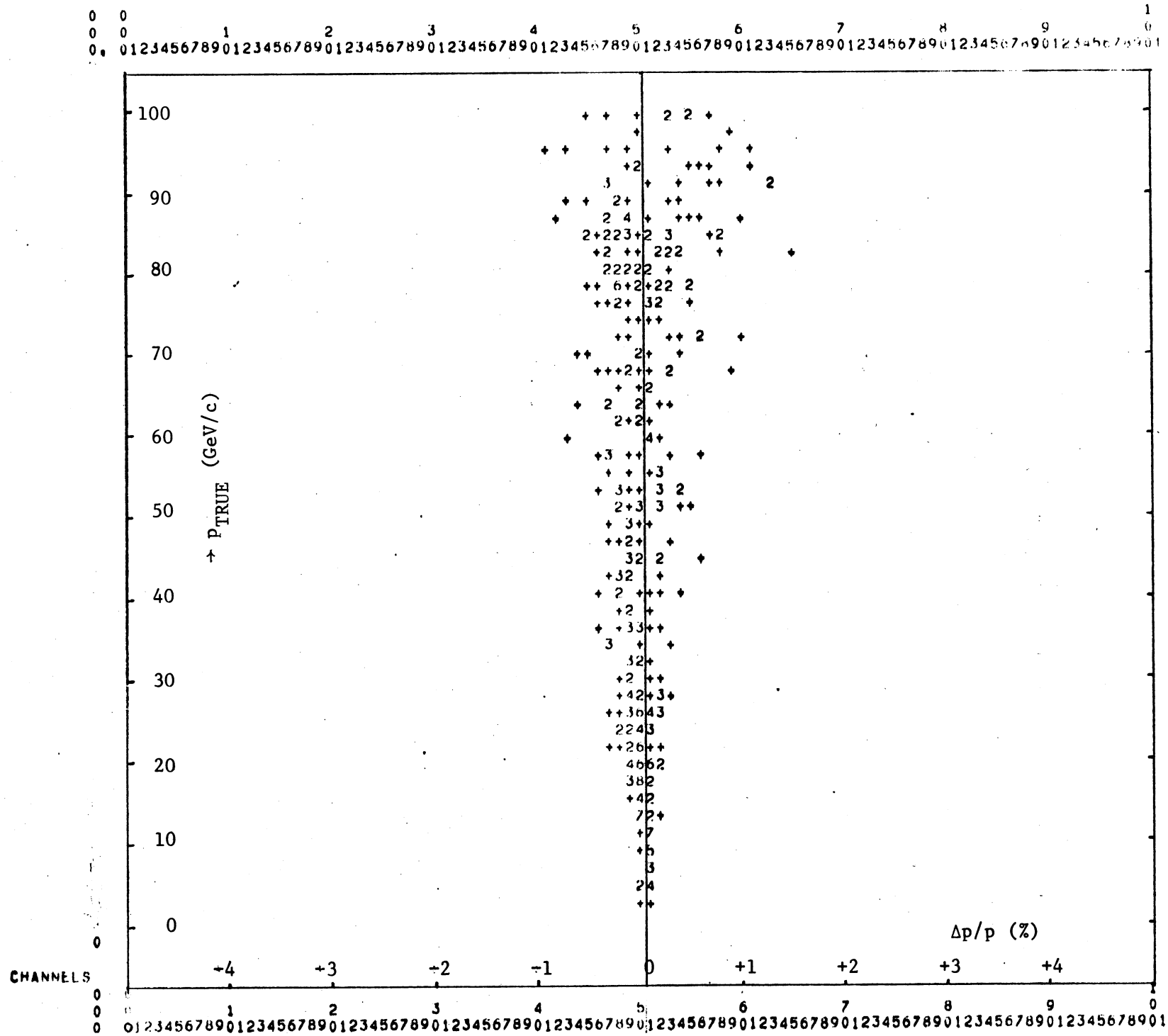

Fig. 5

$\frac{p_{SPLINE} - p_{TRUE}}{p_{TRUE}}$ vs p_{TRUE}

SIMULATED DATA.

HIGHER MOMENTA

Fig. 6. SIMULATED CHAMBER LAYOUT FOR SPLINE TEST

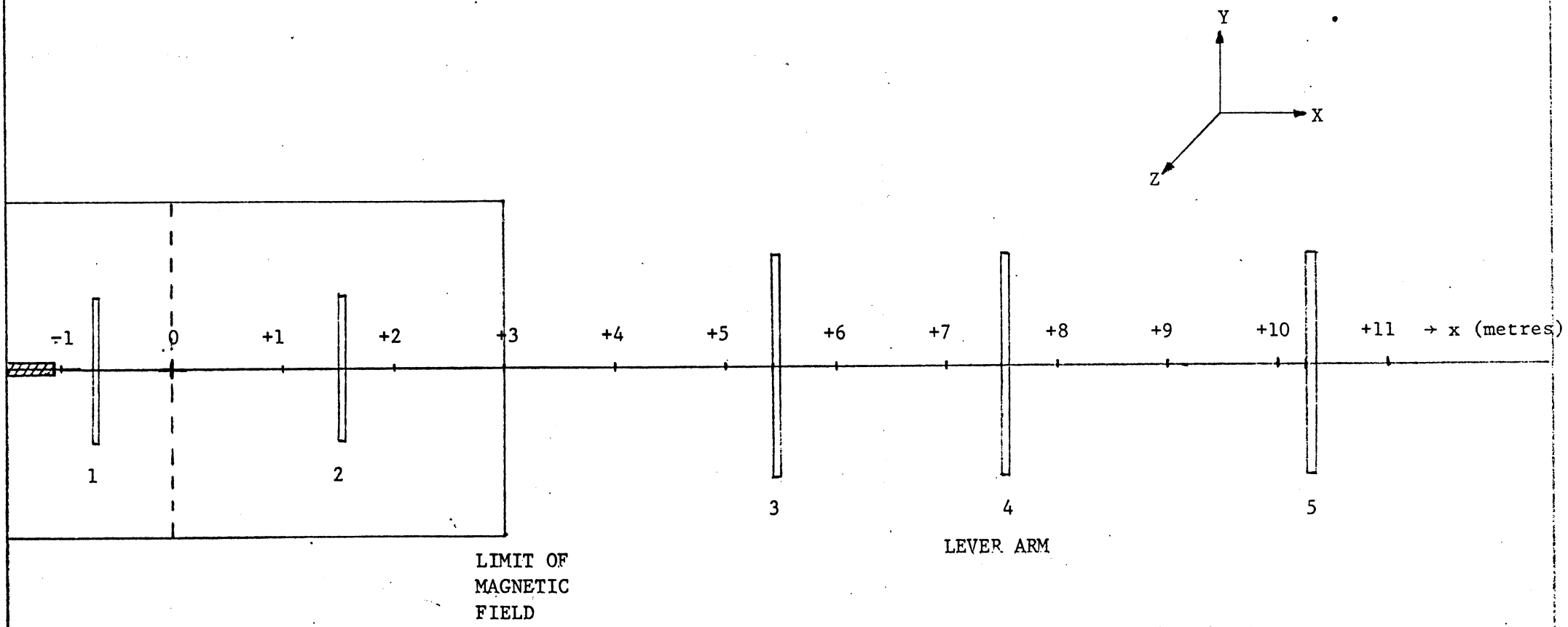

Each module gives a space point (XYZ).

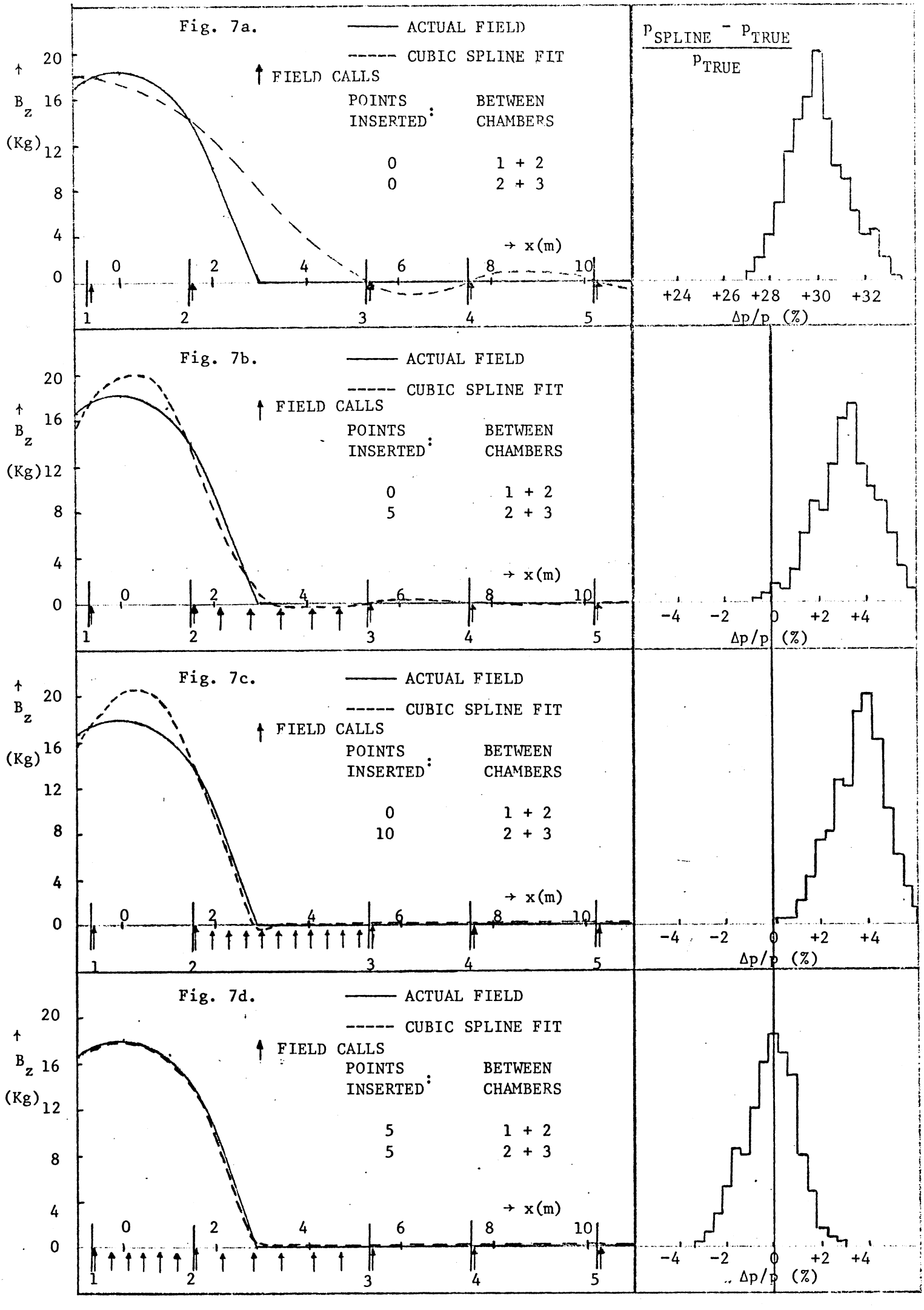
Fig. 7a.
ACTUAL FIELD
CUBIC SPLINE FIT
FIELD CALLS
POINTS INSERTED:
BETWEEN CHAMBERS
0 1 + 2
0 2 + 3
B_z (Kg)
→ x(m)
$\frac{P_{SPLINE} - P_{TRUE}}{P_{TRUE}}$
Δp/p (%)
Fig. 7b.
ACTUAL FIELD
CUBIC SPLINE FIT
FIELD CALLS
POINTS INSERTED:
BETWEEN CHAMBERS
0 1 + 2
5 2 + 3
B_z (Kg)
→ x(m)
Δp/p (%)
Fig. 7c.
ACTUAL FIELD
CUBIC SPLINE FIT
FIELD CALLS
POINTS INSERTED:
BETWEEN CHAMBERS
0 1 + 2
10 2 + 3
B_z (Kg)
→ x(m)
Δp/p (%)
Fig. 7d.
ACTUAL FIELD
CUBIC SPLINE FIT
FIELD CALLS
POINTS INSERTED:
BETWEEN CHAMBERS
5 1 + 2
5 2 + 3
B_z (Kg)
→ x(m)
Δp/p (%)